Cell. Mol. Life Sci. (2010) 67:135–145
DOI 10.1007/s00018-009-0171-7

Cellular and Molecular Life Sciences

RESEARCH ARTICLE

Inactivation of the proximal NPXY motif impairs early steps in LRP1 biosynthesis

Sara M. Reekmans · Thorsten Pflanzner · Philip L. S. M. Gordts · Simone Isbert · Pascale Zimmermann · Wim Annaert · Sascha Weggen · Anton J. M. Roebroek · Claus U. Pietrzik

Received: 10 June 2009 / Revised: 24 September 2009 / Accepted: 5 October 2009 / Published online: 25 October 2009

Abstract The proximal NPXY and distal NPXYXXL motifs in the intracellular domain of LRP1 play an important role in regulation of the function of the receptor. The impact of single and double inactivating knock-in mutations of these motifs on receptor maturation, cell surface expression, and ligand internalization was analyzed in mutant and control wild-type mice and MEFs. Single inactivation of the proximal NPXY or in combination with inactivation of the distal NPXYXXL motif are both shown to be associated with an impaired maturation and premature proteasomal degradation of full-length LRP1. Therefore, only a small mature LRP1 pool is able to reach the cell surface resulting indirectly in severe impairment of ligand internalization. Single inactivation of the NPXYXXL motif revealed normal maturation, but direct impairment of ligand internalization. In conclusion, the proximal NPXY motif proves to be essential for early steps in the LRP1 biosynthesis, whereas NPXYXXL appears rather relevant for internalization.

Keywords Internalization motif · LRP1 · Endocytosis · Maturation · NPXY motif · Proteasomal degradation · Intracellular domain · Lipoprotein receptor

Introduction

The Low Density Lipoprotein Receptor-related Protein 1 (LRP1) is a multifunctional endocytic receptor belonging to the LDL receptor family. It binds a variety of unrelated ligands e.g., ApoE containing lipoproteins, proteases and complexes of protease–protease inhibitors, Amyloid Precursor Protein (APP) and growth factors. LRP1 functions

S. M. Reekmans, T. Pflanzer and P. L. S. M. Gordts are co-first authors. A. J. M. Roebroek and C. U. Pietrzik are co-last authors.

Electronic supplementary material The online version of this article (doi:10.1007/s00018-009-0171-7) contains supplementary material, which is available to authorized users.

S. M. Reekmans · P. L. S. M. Gordts · A. J. M. Roebroek (✉)
Laboratory for Experimental Mouse Genetics,
Center for Human Genetics, KU Leuven,
Herestraat 49, bus 602, 3000 Leuven, Belgium
e-mail: anton.roebroek@med.kuleuven.be

P. Zimmermann
Laboratory for Signal Integration in Cell Fate Decision,
Center for Human Genetics, KU Leuven, Leuven, Belgium

W. Annaert
Laboratory of Membrane Trafficking,
Center for Human Genetics, KU Leuven, Leuven, Belgium

S. M. Reekmans · P. L. S. M. Gordts · A. J. M. Roebroek
Laboratory for Experimental Mouse Genetics,
Department of Molecular and Developmental Genetics,
VIB, Leuven, Belgium

W. Annaert
Laboratory of Membrane Trafficking, Department of Molecular and Developmental Genetics, VIB, Leuven, Belgium

S. Weggen
Department of Neuropathology, Heinrich-Heine-University, Düsseldorf, Germany

T. Pflanzner · S. Isbert · C. U. Pietrzik (✉)
Molecular Neurodegeneration, Department of Physiological Chemistry and Pathobiochemistry,
University Medical Center of the Johannes Gutenberg-University Mainz, Duesbergweg 6,
55099 Mainz, Germany
e-mail: pietrzik@uni-mainz.de

not only as an important endocytic cargo or clearing receptor, but it is also involved as (co-)receptor in signal transduction [1–3]. As such, LRP1 participates in a number of diverse (patho)physiological processes such as lipid metabolism, Alzheimer's disease, and atherosclerosis.

LRP1 is synthesised as a 600-kDa type I transmembrane protein which during transit to the cell surface is processed by furin [4] into a large 515-kDa α- and a smaller 85-kDa *β*-subunit in the *trans*-Golgi network (TGN) [5]. The *β*-subunit contains a small extracellular domain, a transmembrane domain and an intracellular domain, and stays after furin cleavage non-covalently connected to the larger α-subunit. The intracellular domain of LRP1 contains many potential motifs, postulated to have a role in basolateral sorting, internalization, recycling of the receptor, and binding of several different adaptor proteins: two NPXY motifs, the distal one overlapping with an YXXL internalization motif, two di-leucine internalization motifs and several serine, threonine and tyrosine phosphorylation sites. Rather than the NPXY and di-leucine motifs, the YXXL was shown to be the dominant endocytosis signal in LRP1 mini-receptor constructs [6]. In addition, both NPXY motifs appeared to be differentially important in basolateral sorting of mini-LRP1 in polarized epithelial cells [7, 8]. Both the proximal NPXY and distal NPXYXXL motifs are capable of interacting with cytoplasmic adaptors and scaffold proteins, like DAB1, FE65, JIP1, PSD-95, SHC, Snx17, and CED-6/GULP [9–16]. Although most of these proteins have been shown to bind only the distal NPXYXXL motif in the LRP1 intracellular domain, FE65 can bind both motifs, and Snx17 is the only interacting protein so far identified to bind exclusively to the proximal NPXY motif [9, 14, 15]. Furthermore, phosphorylation of the LRP1 intracellular domain is believed to regulate association with adaptor molecules as well as endocytosis [12, 15, 17–20]. Thus, association with specific adaptor molecules in combination with LRP1 intracellular domain phosphorylation is believed to be essential for the differentiation of LRP1 function in cargo transport or in signaling pathways upon binding of different ligands to the receptor. The diversity of extracellular and intracellular LRP1 binding partners highlights its multiple functions in physiological and pathophysiological processes [21].

Most of the above mentioned findings were obtained in vitro in an overexpression system with LRP1 mini-receptors with a largely reduced extracellular domain, since experimental research on LRP1 function in vivo by a genetic approach is impaired due to the embryonic lethal phenotype of the *Lrp1* knock-out mouse [22, 23]. However, the Cre-LoxP system was successfully used to inactivate *Lrp1* conditionally in order to study different aspects of LRP1 function in vivo [24–27]. In such an approach, complete inactivation of *Lrp1* is triggered in particular tissues or cells. Recently, we described the successful design and application of a recombinase-mediated cassette exchange (RMCE) method to knock-in mutations in regulatory signal motifs in the LRP1 intracellular domain [28]. These knock-in (not classic transgenic) mouse models can be considered as partial *Lrp1* knock-out mouse models, in which presumably only parts of the complex biological functions of endogenous LRP1 are impaired. However, a combination of different knock-in mutations in one mutant mouse is likely expected to reveal cumulated effects. Here, we report on the generation and characterization of an early embryonic lethal mutant *Lrp1* knock-in mouse and derived mouse embryonic fibroblasts (MEFs) with combined inactivation of the proximal NPXY and distal NPXYXXL motifs, showing such a cumulated effect. Biochemical and cell biological characterization of these double mutant MEFs in comparison with previously described single mutant and wild-type MEFs [28] reveal the novel finding that the proximal NPXY motif is essential for early steps in the biosynthesis preceding the generation of mature LRP1 in the TGN.

Materials and methods

Primary antibodies

Rabbit antibody 1704, recognizing the C terminus of the LRP1 protein, and rabbit antibody 2.2, detecting the α-subunit, were described previously [28, 29]. A mouse antibody directed against *β*-actin (Sigma-Aldrich) or a polyclonal antibody against ERK1/2 (Cell Signaling Technology) were used as loading control in western blot analysis. Furthermore, for western blot analysis of cell fractionation samples, the following antibodies were used: antibodies against Early Endosomal Antigen 1 (EEA1), GM130 and Syntaxin 6 from BD Transduction Laboratories, antibodies against Ribophorin 1 and Rab5 (kindly provided by R. Schekman, University of Berkeley, USA and R. Jahn, Max Planck Institute for Biophysical Chemistry, Göttingen, Germany, respectively).

Application of RMCE, generation of *Lrp1* knock-in mice and derivation of MEFs

Construction of plasmids for application of RMCE in ES cells was previously described in detail [28]. The same primers used to introduce the proximal NPXY (NPXY1; NPTY → AATA) and distal NPXYXXL (NPXY2; NPVYATL → AAVAATL) single mutations were successively used in a QuickChange site-directed mutagenesis kit (Stratagene) to obtain a plasmid construct carrying both mutations (NPXY1+2). Application of RMCE in ES cells

to knock-in the mutation into the endogenous *Lrp1* allele of the mouse, generation of knock-in mice, and derivation of mouse embryonic fibroblasts from an embryonic day 12.5 (E12.5) embryo were as described [28]. For comparative reasons, these novel MEFs were analyzed together with previously derived and described LRP1 (knock-in) MEFs: wild-type LRP1, LRP1–NPXY1 knock-in and LRP1–NPXY2 knock-in [28]. Of two previously described different LRP1–NPXY1 knock-in MEF cell lines, only the one with the relatively high LRP1 expression was used. As LRP1 knock-out control MEF cell line, PEA-13 cells were used [30]. All MEF cell lines were cultured in DMEM-F12 (Invitrogen), supplemented with 10% FCS, 100 U/ml penicillin and 0.1 mg/ml streptomycin, at 37°C and 5% CO_2. The research was approved by the Institutional Animal Care and Research Advisory Committee of the KU Leuven.

Immunoblotting

Expression of full-length LRP1 (LRP1 fl), LRP1-α, and LRP1-β was analyzed in MEF cell line lysates and homogenized cut-of head regions of E12.5 LRP1 single NPXY1 and NPXY1+2 double mutant and wild-type control littermate embryos. For MEF cell lines (20 µg protein) and for embryonic tissue (40 µg protein), total cell lysates were analyzed. Proteins were separated on 4–12% bis–tris gels (Invitrogen) under denaturing, reducing conditions and transferred to nitrocellulose membranes (GE Healthcare). Membranes were blocked in tris-buffered saline containing 0.1% Tween 20 and 5% milk. For detection of LRP1, antibodies 2.2 and 1704 were used. Secondary antibodies linked to horseradish peroxidase were visualized by ECL reagent (GE Healthcare).

Cell fractionation experiments

Cell fractionation was carried out as described previously with some modifications [31]. All steps of the fractionation protocol were carried out at 4°C. Briefly, confluent MEFs on a 600-cm^2 tissue culture plate were washed and scraped in ice-cold PBS and centrifuged for 5 min at 650*g* (4°C). The pellet was resuspended in 1 ml homogenization buffer [10 mM triethanolamine; 10 mM acetic acid; 250 mM sucrose; 1 mM EDTA; 1 mM DTT (pH 7.4)] and homogenized by a ball-bearing cellcracker (clearance 10 µm). Protease inhibitors were added to the homogenate, followed by centrifugation for 10 min at 425*g* (4°C). Then, the post-nuclear supernatant (PNS) was collected and loaded carefully on top of a preformed continuous 10–24% nycodenz gradient. After loading the PNS on top of the gradient, the tube was filled to the top with homogenization buffer. The gradient was centrifuged for 1.45 h at 169,044*g* in an SW41 rotor. Twelve 1-ml fractions were collected from the top to the bottom of the gradient using a fraction collector. For each fraction, equal volumes (83 µl) of protein were used for further processing by western blot analysis.

Analysis of LRP1 biosynthesis in pulse-chase experiments

Confluent cultures of the MEF cell lines were starved for 1 h in DMEM deprived of methionine/cysteine (Met/Cys), and subsequently pulse labeled for 1 h with Met/Cys-free DMEM, supplemented with 150 µCi/ml [^{35}S]Met/Cys. Cells were immediately lysed or chased for 6, 12, 24, or 48 h. LRP1 was immunoprecipitated overnight at 4°C with the 1704 antibody. The beads were washed three times with 1% NP40 lysis buffer (50 mM Tris–HCl, 150 mM NaCl, 0.02% NaN_3, 1% Nonidet P40) and boiled in LDS sample buffer. Bound proteins were separated on 4–12% bis–tris gels (Invitrogen) under denaturing, reducing conditions and dried on Whatman paper. Quantification was done using a phosphor-imager (Fujifilm BAS 1800) and AIDA software.

Deglycosylation

Whole protein extracts of the MEF cell lines were deglycosylated with Endoglycosidase H (EndoH) or *N*-glycosidase F (*N*-glycF) as described by the manufacturer (Roche Diagnostics). Briefly, 20 µg of protein (1 µg/µl) was incubated for 10 min at 70°C in 20 µl digestion buffer [20 mM sodium phosphate (pH 6), 0.2% SDS, 1% β-mercaptoethanol and protease inhibitors]. Next, EndoH (10 mU) or *N*-GlycF (10 mU) was added and the samples were incubated overnight at 37°C. Samples were analyzed by western blotting (3–8% tris–acetate gels, Invitrogen) with the 1704 antibody.

Proteasomal degradation

Cells were radiolabeled as described above, in the presence or absence of 50 µM MG132 (Sigma-Aldrich). Cells were subsequently chased for 4 h in normal growth medium containing MG132 or DMSO (solvent for MG132). Analysis was performed as described for the pulse-chase experiments. The impact of MG132 on the full-length LRP1 expression levels in comparison to untreated controls was determined for each of the MEF cell lines.

Cell surface biotinylation experiments

MEF cells were grown to near confluence in 10-cm dishes and washed twice with ice-cold PBS. Cells were incubated for 30 min in ice-cold borate buffer containing 0.5 mg/ml EZ-link Sulfo NHS-LC-LC-Biotin (Pierce Protein Research

Products). Dishes were washed 4 times with ice-cold PBS containing 50 mM NH_4Cl to quench any unconjugated biotin. Cells were lysed in 600 µl 1% NP40 lysis buffer containing protease inhibitors and 400 µg of protein was precipitated with streptavidin beads overnight at 4°C. Beads were washed twice in NP40 lysis buffer and subsequently incubated in LDS sample buffer. Samples were boiled for 10 min at 95°C and the bound material was analyzed by SDS–PAGE and western blotting using the 1704 antibody.

Endocytosis assay

The endocytosis assay was adapted from the procedure performed by Dedieu et al. [32]. Briefly, subconfluent MEFs were washed twice with PBS and incubated for 1 h at 37°C in fresh serum-free medium containing 50 µg/ml FITC-labeled human α_2M (Biomac) alone, or together with 1 µM RAP, in the presence of 100 µM chloroquine (Sigma-Aldrich) to inhibit lysosomal activity. Human RAP was expressed in bacteria as a fusion protein with glutathione *S*-transferase and was purified as described previously [33]. Cells were next washed three times with ice-cold PBS and the remaining surface bound FITC-α_2M was removed by incubating the cells for 2 min with PBS containing 10 U/ml heparin on ice. Finally the cells were solubilised in ice-cold lysisbuffer [50 mM NaF, 1 mM Na_2EDTA, 1 mM EGTA, 20 µM phenylarsine oxide, 5 mM Na_3VO_4, 1% Triton X-100 and proteinase inhibitors (Complete^{TM}, Roche Applied Science)]. Cell homogenates were centrifuged for 20 min at 15,000*g* and the supernatant was collected to measure the intracellular fluorescence and the protein concentration. The amounts of α_2M internalized (RFU/mg protein) are expressed as mean + SEM of at least three independent experiments performed in duplicate.

Statistics

For analysis of endocytosis, statistical significance between groups was determined by the Kruskal–Wallis and Mann–Whitney rank sum tests using STATISTICA version 6 software (StatSoft). Pulse-chase and proteasome degradation experiments were analyzed using a one-way ANOVA coupled with a Newman–Keuls post-hoc test in which $P < 0.05$ was the minimum requirement for a statistically significant difference. Statistical analysis was performed with GraphPad Prism 4 software (GraphPad).

Results

Combined inactivation of the proximal NPXY and distal NPXYXXL motifs results in embryonic lethality between E10.5 and E13.5

Single inactivation of the proximal NPXY (indicated by NPXY1 or n1) motif resulted in perinatal lethality caused by fetal liver degeneration observed at the earliest at E15.5, whereas inactivation of the distal NPXYXXL (indicated by NPXY2 or n2) revealed initially no clear phenotype [28]. Only recently, it was shown in an LDLR-deficient background that this motif contributes to the protective role of LRP1 with regard to atherosclerosis [34]. However, we hypothesized that combined inactivation of both motifs might result in a phenotype at least as dramatic as the single inactivation of the NPXY1 motif. Indeed, comparative analysis of the relative number of homozygous NPXY1 and NPXY1+2 (n1+2) double mutant embryos, present in different embryonic stages resulting from hybrid crosses, revealed embryonic lethality between E10.5 and E13.5 for the NPXY1+2 double mutant, whereas for the NPXY1 mutant, lethality occurred later between E14.5 and birth (Table 1) [28]. The wide developmental window of the embryonic lethality observed for the NPXY1+2 double mutant is characterized by the presence of living mutant embryos, which appeared both macroscopically normal or differentially delayed in development, and already dead embryos in the stages E10.5, E11.5 and E12.5 (data in Electronic Supplementary Material). A number of delayed or dead embryos showed internal hemorrhages. However, these hemorrhages were rare and inconsistent and therefore seem not systematically associated with the death of the embryos. Histological analysis of a macroscopically normal E12.5 embryo of double mutant *Lrp1* knock-in mice revealed no anomalies, not even in the liver, which could

Table 1 Relative presence of living homozygous mutant *Lrp1* knock-in offspring in a hybrid cross

	HOM at E10.5	HOM at E11.5	HOM at E12.5	HOM at E13.5	HOM at E14.5	HOM at E16.5	HOM at E18.5	HOM New born
n2	–	–	–	–	–	–	–	27% (38/142)
n1	22% (11/51)	–	–	–	24% (21/86)	16% (22/140)	15% (18/124)	0% (0/72)
n1 + n2	25% (20/79)	13% (9/71)	8% (7/86)	0% (0/42)	–	–	–	0% (0/121)

Number of homozygous mutant embryos versus total number of embryos between parentheses. Data for n1 from [28], data for n2 not previously published

have explained its expected death only 1 day later (data not shown). The observed phenotype is reminiscent of the observed embryonic lethal phenotype for the full LRP1 knock-out mice allele [22, 23]. Therefore, we suggest that the NPXY1+2 double mutant mouse phenocopies the *Lrp1* full knock-out mouse.

In NPXY1 and NPXY1+2 mutants, steady state levels of full-length LRP1 are normal whereas steady state levels of mature LRP1 are severely reduced

The lethal phenotypes of the NPXY1 and NPXY1+2 LRP1 knock-in mice point towards a severe impairment of the function of LRP1 by these inactivating mutations in the LRP1 intracellular domain. To unravel the mechanism behind the impact of the NPXY mutations on the functioning of the LRP1 receptor, we studied the steady state expression level of LRP1 in all intracellular domain knock-in mutants in comparison to wild-type control in MEF cell lines derived from each mutant mouse line. Since LRP1 is cleaved in the *trans*-Golgi compartment by furin, western blot analyses of cell lysates reveal different processing products like full-length LRP1, furin-cleaved LRP1 α-chain and *β*-chain (Fig. 1a). Total protein extracts of MEF cell lines were analyzed with an antibody recognizing the C terminus of the LRP1 *β*-subunit and as such also recognizing the C terminus of the full-length, immature form of the protein. These analyses revealed that steady state levels of the *β*-subunit, representative for mature LRP1, are severely reduced in the NPXY1 and NPXY1+2, but not in the NPXY2 mutant MEFs (Fig. 1b; LRP1-*β*), whereas steady state levels of full-length, immature, LRP1 seem unaffected in all three mutants (Fig. 1b; LRP1 fl). Furthermore, reduction of the *β*-subunit level in the NPXY1+2 double mutants appeared to be even more pronounced than in the NPXY1 mutant MEFs. Analyses with an antibody recognizing both the α-subunit and full-length LRP1 also indicated that the α-subunit amount is severely reduced in the two MEF cell lines with the NPXY1 and NPXY1+2 mutations (Fig. 1b; LRP1 fl + LRP1-α). The signals obtained with this antibody represent the unchanged steady state levels of full-length LRP1 (Fig. 1b; LRP1 fl) as well as the co-migrating α-subunit. Thus, the reduction in the signal has to be due to reduction of α-subunit levels. The strong reductions in mature LRP1 expression levels were not only found in the NPXY1 and NPXY1+2 knock-in MEF cell line, but also in embryonic homogenates containing predominantly brain tissue. Western blot analysis of homogenates of the head region of E12.5 embryos showed a severe reduction in mature LRP1 (Fig. 1c; LRP1-*β*), whereas the levels of full-length LRP1 seemed to be unaffected (Fig. 1c; LRP1 fl). Like for the MEF cell lines, this reduction appeared to be more pronounced in the double NPXY1+2 mutant than in the single NPXY1 mutant.

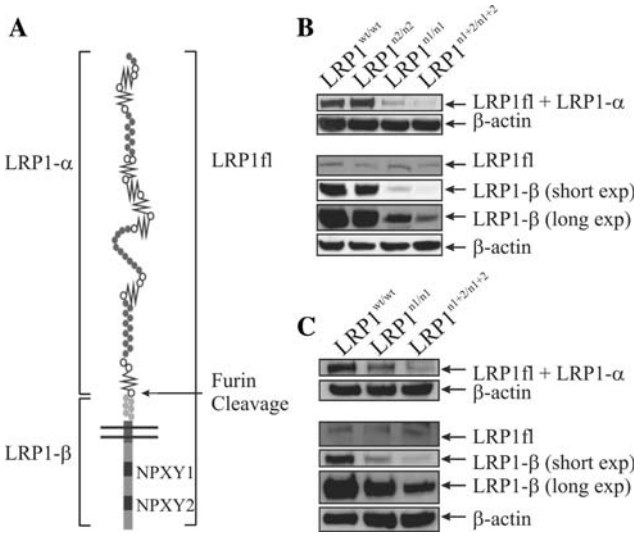

Fig. 1 In NPXY1 and NPXY1+2 mutants, steady state levels of full-length LRP1 are normal whereas steady state levels of mature LRP1 are severely reduced. **a** Schematic representation of immature full-length LRP1 and the mature LRP1-α and LRP1-*β* subunits after furin cleavage. **b**,**c** Total protein extracts of LRP1 mutant MEFs (**b**, 20 μg) or cut-of-head regions of E12.5 embryos (**c**, 40 μg) were analyzed on western blot with antibodies 1704 (LRP1 fl and LRP1-*β*) and 2.2 (LRP1 fl + LRP1-α). A mouse antibody against *β*-actin was used for control of equal loading

The small mature LRP1 pool in the NPXY1 and NPXY1+2 mutants is in contrast to wild-type predominantly present in endosomal fractions only

In NPXY1 and NPXY1+2 mutants, a small amount of full-length LRP1 is cleaved correctly (Fig. 1b, c; LRP1-*β*). Therefore, we investigated whether this small amount of mature mutant LRP1 is present in the same subcellular compartments as mature wild-type LRP1. Cell fractionation experiments revealed that mature wild-type LRP1 has a bimodal subcellular distribution with the largest amounts of mature LRP1 apparently present in the *cis*-Golgi to TGN fractions (GM130 and Syntaxin 6) and the endosomal fractions (EEA1 and Rab5), which is clearly evident from the LRP1-*β* distribution (Fig. 2a; LRP1-*β*). Due to the large overlap in TGN and *cis*-Golgi fractions, actual presence of mature LRP1 in the *cis*-Golgi cannot be excluded. Analysis of glycosylation patterns (see below), however, indicates that mature wild-type LRP1 should predominantly be present in the TGN and more downstream compartments. Nevertheless, the smaller amounts of mature NPXY1 and NPXY1+2 mutant LRP1 show a unimodal distribution. LRP1-*β* is abundant within the endosomal fractions only (Fig. 2b, c; LRP1-*β*). So, the subcellular distribution of mature mutant NPXY1 and

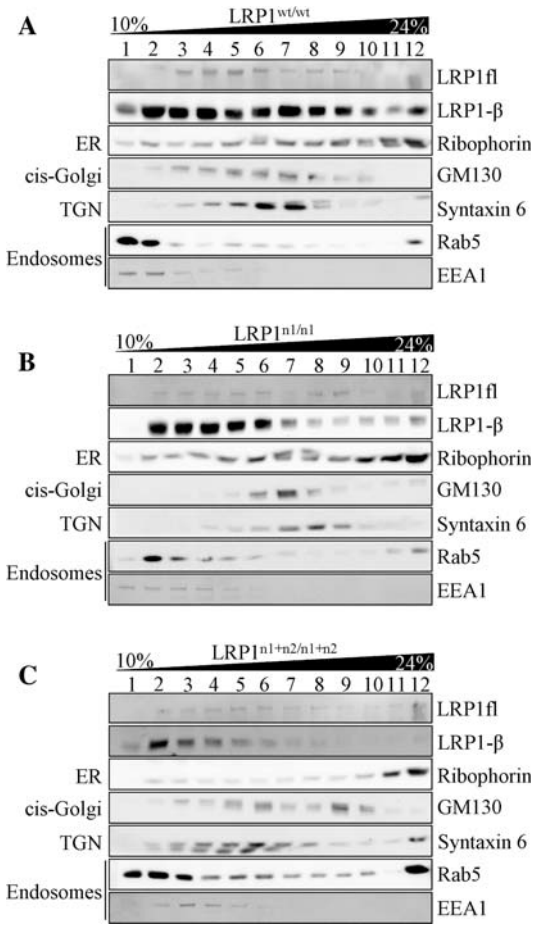

Fig. 2 The small mature LRP1 pool in the NPXY1 and NPXY1+2 mutants is in contrast to wild-type predominantly present in endosomal fractions only. Western blot analysis of fractionated MEFs using a 10–24% nicodenz gradient. Co-distribution of marker proteins for different subcellular compartments (ER/Ribophorin, *cis*-Golgi/GM130, TGN/Syntaxin 6, endosomes/Rab5 and EEA1) and LRP1 fl and LRP1-β. Detection of LRP1 fl and LRP1-β using the 1704 antibody. **a** Wild-type, **b** NPXY1, **c** NPXY1+2

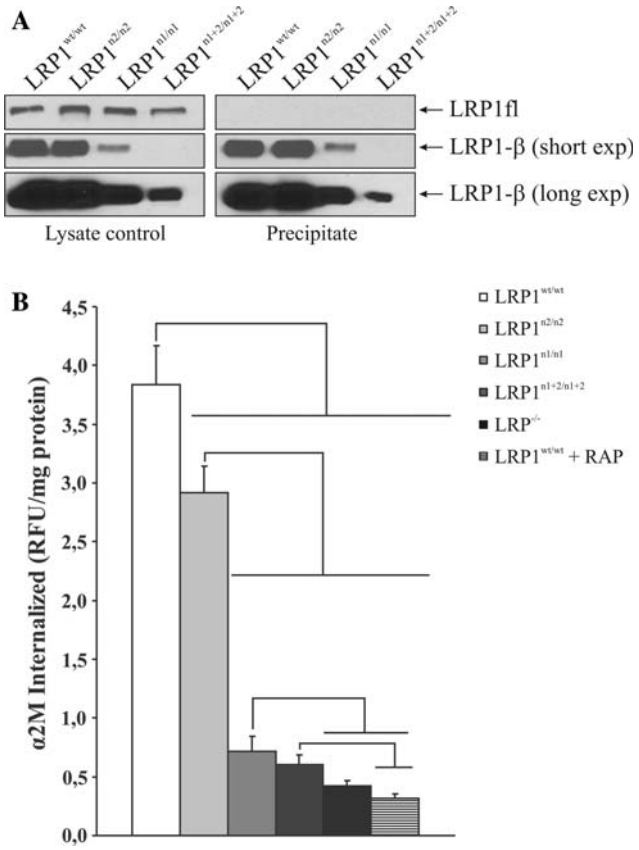

Fig. 3 Cell surface expression of LRP1 and decreased endocytosis rates in the NPXY mutants. **a** Biotinylated cell surface proteins after precipitation from the whole cell lysate with streptavidin beads. Detection of LRP1 fl and LRP1-β using the 1704 antibody in lysate control (*left*) and precipitate (*right*). **b** Steady-state internalization of FITC-labeled α_2M from the cell surface was measured for 1 h at 37°C (see "Endocytosis assay"). In this experiment, the uptake of FITC-labeled α_2M expressed as RFU/mg protein was determined. LRP1-mediated endocytosis of FITC-labeled α_2M was inhibited with 500 nM RAP in WT control cells. Results represent the mean + SEM of at least three independent experiments performed in duplicate. Significant differences (P values < 0.05) between the MEF cell lines are indicated

NPXY1+2 LRP1 is different from wild-type. In contrast, full-length, immature LRP is distributed similarly in both mutant and wild-type cells (Fig. 2a–c; LRP1 fl). The fractions containing LRP1 fl correspond likely to compartments preceding the TGN as will become further evident from analysis of the glycosylation patterns (see below).

The presence of only small amounts of mature LRP1 in the NPXY1 and NPXY1+2 mutants at the cell surface results in strongly decreased endocytosis

Western blot analysis of streptavidin precipitates of cell lysates with the C-terminal anti-LRP1 antibody in a cell surface biotinylation experiment confirms the presence of mature NPXY1 and NPXY1+2 mutant LRP1 at the cell surface. These analyses revealed that normally processed LRP1 in the NPXY2 mutant reached the cell surface equally well as WT LRP1 (Fig. 3a, right panel; LRP1-β). The NPXY1 and the NPXY1+2 mutants also showed cell surface expression of mature LRP1, however, severely reduced when compared to WT LRP1 (Fig. 3a, right panel; LRP1-β), with a more pronounced reduction for the double mutant. This reduction is in proportion to the reduction in steady state levels of correctly matured LRP1 (Fig. 3a, left panel; LRP1-β), but anyhow the pool of mature LRP1 of these mutants is indeed also able to reach the cell surface. As expected, full-length, immature LRP1 also present in this analysis in all MEFs at comparable steady state levels (Fig. 3a, left panel; LRP1 fl), did not reach the cell surface (Fig. 3a, right panel; LRP1 fl), since it should be totally cleaved by furin in the TGN. We hypothesize that the

dramatic effect on LRP1 maturation and cell surface expression has a severe impact on endocytosis by LRP1. Therefore, using an endocytosis assay, we analyzed the internalization of FITC-labeled α_2M as measure of endocytosis. As shown in Fig. 3b, the uptake of α_2M by the NPXY mutant MEFs is significantly reduced in comparison with wild-type MEFs. As already reported recently [34], the internalization of α_2M is only to a limited extent reduced in NPXY2. However, internalization by the NPXY1 and NPXY1+2 mutants was almost reduced to background levels observed in LRP1-deficient MEFs and wild-type MEFs, in which the uptake by LRP1 was inhibited by the specific inhibitor RAP. Compared to these RAP-inhibited wild-type MEFs, the NPXY1 and NPXY1+2 reveal only a small but significant uptake above background. The difference between the two mutants is not significant, but there is a tendency that the NPXY1 mutant has a higher endocytosis compared to the NPXY1+2 mutant.

The NPXY1 and NPXY1+2 knock-in mutants show an equal LRP1 production rate but a dramatically decreased half-life compared to wild-type LRP1

To investigate whether the reduced signal of mature LRP1, in the NPXY1 and NPXY1+2 mutants might be due to a reduction in the production rate of the full-length, immature protein, we performed a metabolic labeling experiment. The MEF cell lines were pulse labeled for 1 h with [^{35}S]-Met/Cys, and full-length LRP1 was immunoprecipitated from the cell lysate with the C-terminal antibody. SDS–PAGE analysis of the immunoprecipitates and subsequent autoradiography did not show any obvious differences in the amounts of newly synthesized LRP1 during pulse labeling in the different MEF cell lines (Fig. 4a). To determine the turnover of LRP1 in each knock-in MEF cell line, we performed standard pulse-chase experiments. After pulse labeling of the cells for 1 h, the cells were chased for different time points from 6, 12, 24 to 48 h. During a 24-h chase period, levels of full-length LRP1 in the WT and NPXY2 mutant MEFs did not show a strong decrease, whereas strikingly enough in the NPXY1 and NPXY1+2 mutants, full-length LRP1 levels are already drastically decreased after 6 h (Fig. 4b). Furthermore, the decrease in full-length LRP1 levels in the WT and NPXY2 mutant MEFs seemed to correspond with an increase in β-subunit levels (Fig 4c), already appearing after 6 h. In the NPXY1 and NPXY1+2 mutant MEFs, however, although full-length LRP1 levels decrease very rapidly (Fig. 4b), β-subunit levels (Fig. 4c) never rise above the detection limit, confirming the low steady state levels of the β-subunit observed before (Fig. 1b, c). Determination of the half-life of full-length LRP1 revealed a half-life of approximately 24 h for wild-type and for

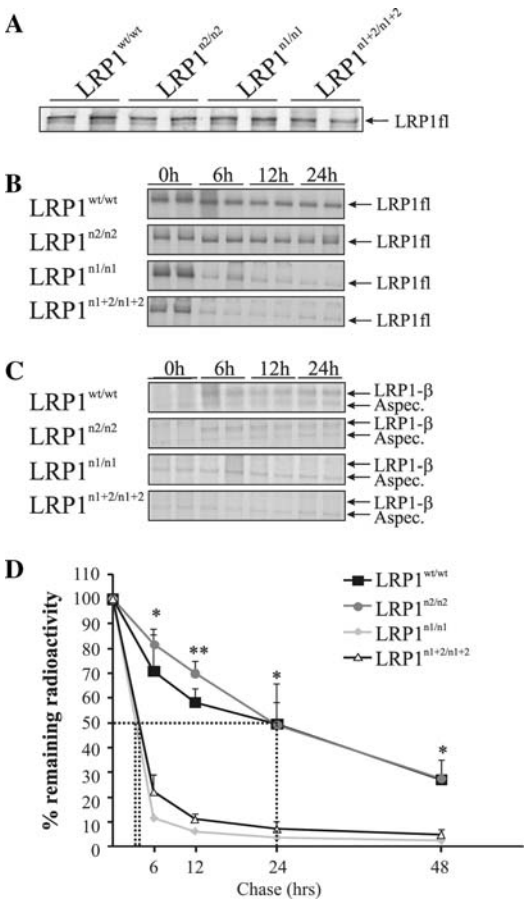

Fig. 4 Turnover of full-length LRP1 is significantly increased in the NPXY1 and NPXY1+2 mutants. **a** Autoradiography of the full-length LRP1 rate of production after a 1 h metabolical [^{35}S] pulse labeling. **b**,**c** Autoradiography of immunoprecipitated LRP1, using the 1704 antibody at chase time points from 0 to 24 h, representing full-length (**b**) and β-subunit LRP1 (**c**). **d** Half-life graph. Data are mean + SEM. $^*P < 0.05$ and $^{**}P < 0.001$: differences between WT or n2 with n1 or n1+2

NPXY2 mutant LRP1 and of approximately 3.5 h for NPXY1 and NPXY1+2 mutant LRP1 (Fig. 4d).

Premature proteasomal degradation preceding maturation is responsible for the reduction of mature LRP1 levels in the LRP1 NPXY1 and NPXY1+2 mutants

In an attempt to clarify the reason of the impaired maturation and increased turnover of LRP1 in the NPXY1 and NPXY1+2 mutants, we first analyzed the glycosylation pattern of full-length and mature LRP1 in the cells. In previous studies, Herz and colleagues demonstrated that LRP1 is synthesized as an *N*-glycosylated, Endoglycosidase H (EndoH) sensitive precursor with a molecular weight of 600 kDa. The proteolytic processing of this precursor occurs at about the same time that the *N*-linked carbohydrates are

converted to the EndoH resistant form in the *trans*-Golgi network [5]. Therefore, we subjected total protein extracts from the different MEF cell lines to EndoH and *N*-glycosidase F (*N*-glycF) digestion and subsequently analyzed them for LRP1 full-length and β-subunit expression using western blot analysis. Neither EndoH, nor *N*-glycF treatment revealed differences in the glycosylation pattern of the different mutants compared to WT LRP1 (Fig. 5a). The complete pool of full-length LRP1 (Fig. 5a; LRP1 fl) in all mutants is EndoH sensitive indicating that indeed this pool resides in the compartments preceding the TGN, whereas the complete β-subunit pool (Fig. 5a; LRP1-β) in all mutants is EndoH resistant indicating that this pool resides in the TGN and subsequent compartments. *N*-glycF treatment was used as a control for complete deglycosylation of the proteins. The deglycosylation data suggest that full-length LRP1 of the NPXY1 and NPXY1+2 mutants can be processed as normal, despite their strong reduction in steady state levels of mature LRP1 (Fig. 5a; LRP1-β). Impaired maturation of full-length LRP1 into mature LRP1 in the TGN, where cleavage of immature LRP1 into mature LRP1 occurs, should be expected to result in accumulation of immature LRP1 in compartments preceding the TGN. This, however, cannot be the explanation, given that steady-state levels of the full-length protein apparently are not higher in these mutants compared to WT MEFs (Figs. 1b and 3a, left panel). We therefore analyzed whether proteasomal breakdown might be involved in the degradation of this immature, 'non-processed' LRP1 pool. An increased proteasomal degradation of LRP1 could also explain the huge difference in turnover between the different MEF cell lines. To analyze this hypothesis, we metabolically labeled the different MEF cell lines for 1 h in the presence or absence of MG132, an inhibitor of the proteasomal degradation. Subsequently, the cells were chased for 4 h in normal growth medium with or without MG132. This treatment revealed that MG132 had only a minor effect on the levels of full-length LRP1 protein in WT and NPXY2 mutant MEFs since the expression level ratio between treated and untreated was close to one (Fig. 5b). However, this expression level ratio between treated and untreated showed a significant increase for the NPXY1 and NPXY1+2 mutant MEFs (Fig. 5b), indicating that indeed a large portion of the full-length pool is degraded by the proteasomal degradation pathway in these cell lines. The significant higher ratio for the NPXY1+2 mutant compared to the ratio for NPXY1 is indicative for a larger portion of the full-length LRP1 pool being degraded in the NPXY1+2 mutant compared to the NPXY1 mutant, resulting in even lower levels of mature LRP1 for the NPXY1+2 mutant compared to the NPXY1 mutant as already shown in other analyses (Figs. 1b and 3a, left panel; LRP1-β).

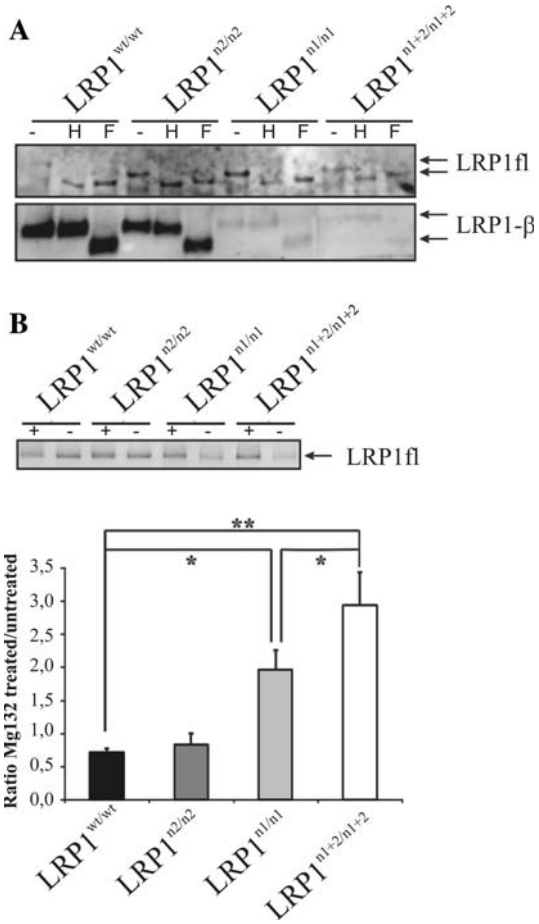

Fig. 5 LRP1 in the NPXY1 and NPXY1+2 mutants is not efficiently transported to the TGN and a large part of the full-length pool is degraded by the proteasome. **a** Detection of LRP1 fl and LRP1-β using the 1704 antibody after EndoH (H) and *N*-GlyF (F) digestion of whole cell lysates. **b** Autoradiography of immunoprecipitated LRP1 using the 1704 antibody, after pulse/chase-labeling (1 and 4 h, respectively) of the cells in the presence (+) or absence (−) of 50 μM MG132. The graph shows the impact of MG132 on the full-length LRP1 expression levels in comparison to untreated controls for each of the MEF, expressed as the ratio between treated and untreated controls. Values are the average of three independent experiments, *error bars* indicate SEM, $*P < 0.05$, $**P < 0.001$

Discussion

As was expected, combined inactivation of both the NPXY1 and NPXY2 motifs resulted in a phenotype more severe than single inactivation of the NPXY1 motif. Additional inactivation of NPXY2 is responsible for an earlier lethal phenotype. Previous results indicated that NPXY1 can apparently compensate for loss of NPXY2 but not the other way round [28]. However, the present analysis of the combined inactivation suggests that the NPXY2 domain is partly able to complement for the loss of the NPXY1 domain, resulting in a shift of embryonic lethality

towards a later stage of development in the NPXY1 mutant compared to the double mutant. The observed lethal phenotype within a broad developmental window of E10.5 to E13.5 of the double mutant is reminiscent of the lethal phenotype of the *Lrp1* full knock-out allele, as documented by Herz and colleagues [22, 23]. It should be noted that the reported description of the *Lrp1* full knock-out phenotype is limited to an embryonic survival table and macroscopical analysis of the embryos, as presented here for the NPXY1+2 double mutant embryos. So further detailed, e.g., morphological and histological analyses of the lethal phenotype of the NPXY1+2 mutant embryos for comparative reasons are not considered as being relevant for the presented study here. Especially, also, because, due to the lethality in a wide developmental window and the large number of different LRP1 ligands potentially involved, the actual physiological pathways implicated in the death of the NPXY1+2 mutant (and also the *Lrp1* full knock-out embryos) are likely manifold and require extensive additional studies on mutant embryos, which are beyond the scope of this study. The obtained results, however, indicate that combined inactivation of both NPXY motifs most likely phenocopies the *Lrp1* knock-out mice due to a presumably almost complete loss of the biological function of this receptor in this mutant mouse model as discussed below.

Our biochemical and cell biological analysis of the different LRP1 knock-in MEFs revealed a reduction in levels of mature LRP1 in case the NPXY1 motif was mutated (NPXY1 and NPXY1+2). Analysis of the synthesis of endogenous full-length immature precursor LRP1 in mutant MEFs showed no apparent differences in the amount of newly synthesized LRP1 during pulse labeling or steady state levels compared to wild-type MEFs. Steady state levels of the β-subunit, representative for mature LRP1, on the contrary are severely reduced in the NPXY1 and NPXY1+2 mutants, with an even more pronounced reduction in the latter. Deglycosylation experiments revealed that the majority of the full-length LRP1 pool in the NPXY1 and NPXY1+2 mutants is unable to reach the TGN, where furin cleavage of LRP1 occurs. Furthermore, the immature 'non-cleavable' LRP1 pool does not accumulate in the cell but is rather degraded by the proteasome. The mature LRP1 pool is very small in the NPXY1 mutant MEFs and even further reduced in NPXY1+2 mutant MEFs. Since the surface amount of mature LRP1 in the double mutant NPXY1+2 MEFs is extremely low, and actual receptor activity was only detectable just above background, we hypothesize that the double mutant mouse is indeed an almost complete phenocopy of the full *Lrp1* knock-out animal. For the single NPXY2 mutant, LRP1 processing in MEFs appears not to be different from wild-type LRP1 although endocytosis is to a certain extent impaired in NPXY2 mutant MEFs due to a direct effect on internalization. The observed impairment of internalization in the single NPXY1 mutant, like for the NPXY1+2 mutant, can surely be contributed to an indirect impact of the mutation via its effect on maturation. The mature pool of the NPXY1 mutant which reaches the cell surface is able to internalize. However, due to the extreme differences in cell surface expression between wild-type and NPXY1, the relative contributions of defective maturation and a potential direct effect on internalization cannot be determined in our fluorescence-labeled α_2M uptake assay.

Previously, the involvement of the proximal NPXY and distal NPXYXXL motifs in basolateral sorting, internalization, and recycling was revealed by overexpression studies of LRP1 mini-receptors with a α-subunit and mutants thereof strongly reduced in size [6–8, 15]. Apparently, the YXXL motif in the NPXYXXL (NPXY2) double motif is the dominant motif for endocytosis. In agreement with this, our analysis of internalization by the NPXY2 mutant also revealed impairment of uptake, likely via inactivation of the YXXL motif. The difference in subcellular localization of normal levels of mature wild-type LRP1 (TGN and endosomes) and the reduced levels of mature NPXY1 and NPXY1+2 mutant LRP1 (predominantly endosomes only) is probably the result of disturbance of the interaction between the NPXY1 motif and Snx17, a protein known to interact with the NPXY1 motif of LRP1, which plays an important role in endosomal sorting and recycling of mature LRP1 [8, 15].

The important novel finding of the present study, however, is that the NPXY1 motif of LRP1 is essential for early steps in the biosynthesis preceding the generation of mature LRP1. This novel function of the NPXY1 motif in LRP1 could apparently not be unmasked in an experimental setting using overexpression of mutant mini-receptor-constructs [6–8], and underscores the relevance of tackling the elucidation of the function of a protein or a protein domain by different approaches including knock-down, knock-out, knock-in and overexpression analysis. So, based upon our novel knock-in data, we speculate that the NPXY1 motif of LRP1 is very important in early steps in biosynthesis of LRP1 in ER/*cis*-/medial-Golgi compartments. However, because the only two interacting proteins shown so far to bind to the NPXY1 motif, Snx17 (see above) and FE65 (bridging of LRP1 and APP C termini at the cell surface), seem to be involved in downstream processes [8, 14, 15], the proteins relevant for interaction with the NPXY1 domain and regulating early biosynthesis steps are still illusive. In line with our findings, Nahari and colleagues [35] recently showed that a transplanted NPXY sequence in the cytosolic domain of the erythropoietin receptor enhanced maturation and cell surface expression of this receptor, which normally shows

only slow exit out of the ER due to inefficient folding mediated by the receptor extracellular domain. So, potentially, the inactivation of the NPXY1 domain has an impact on the velocity by which full-length LRP1 exits the ER and transverses the *cis*- and medial-Golgi resulting in an increased exposure of full-length LRP1 to the protein degradation machinery of the proteasome.

In conclusion, the results presented in this study highlight a novel important role of, especially, the NPXY1 domain in early steps of LRP1 biosynthesis. This novel role might even be relevant for other lipoprotein receptors and unrelated receptors sharing NPXY motifs.

Acknowledgments This work was supported by the "Fonds voor Wetenschappelijk Onderzoek Vlaanderen (FWO)", SAO-FRMA/2004/2006 and VIB to A.R., the Concerted Actions Program (GOA/2006-2010) to P.Z. and A.R., VIB, the SAO-FRMA/2006 and IAP P6/43 to W.A. and the "Deutsche Forschungsgemeinschaft" Grant Pi 379 3-3 and "Bundesministerium für Forschung und Bilding" Grant 01GI0719 to C.P.. The research was also funded by PhD grants of the Institute for the Promotion of Innovation through Science and Technology in Flanders (IWT-Vlaanderen) to S.R. and P.G. We thank Annick Lauwers, Nathalie Feyaerts and Leen Verbeek for technical assistance.

References

1. Strickland DK, Ranganathan S (2003) Diverse role of LDL receptor-related protein in the clearance of proteases and in signaling. J Thromb Haemost 1:1663–1670
2. Lillis AP, Mikhailenko I, Strickland DK (2005) Beyond endocytosis: LRP function in cell migration, proliferation and vascular permeability. J Thromb Haemost 3:1884–1893
3. May P, Herz J, Bock HH (2005) Molecular mechanisms of lipoprotein receptor signalling. Cell Mol Life Sci 62:2325–2338
4. Willnow TE, Moehring JM, Inocencio NM, Moehring TJ, Herz J (1996) The low-density-lipoprotein receptor-related protein (LRP) is processed by furin in vivo and in vitro. Biochem J 313:71–76
5. Herz J, Kowal RC, Goldstein JL, Brown MS (1990) Proteolytic processing of the 600 kD low density lipoprotein receptor-related protein (LRP) occurs in a *trans*-Golgi compartment. EMBO J 9:1769–1776
6. Li Y, Marzolo MP, van Kerkhof P, Strous GJ, Bu G (2000) The YXXL motif, but not the two NPXY motifs, serves as the dominant endocytosis signal for low density lipoprotein receptor-related protein. J Biol Chem 275:17187–17194
7. Marzolo MP, Yuseff MI, Retamal C, Donoso M, Ezquer F, Farfan P, Li Y, Bu G (2003) Differential distribution of low-density lipoprotein-receptor-related protein (LRP) and megalin in polarized epithelial cells is determined by their cytoplasmic domains. Traffic 4:273–288
8. Donoso M, Cancino J, Lee J, van Kerkhof P, Retamal C, Bu G, Gonzalez A, Caceres A, Marzolo MP (2009) Polarized traffic of LRP1 involves AP1B and SNX17 operating on Y-dependent sorting motifs in different pathways. Mol Biol Cell 20:481–497
9. Trommsdorff M, Borg JP, Margolis B, Herz J (1998) Interaction of cytosolic adaptor proteins with neuronal apolipoprotein E receptors and the amyloid precursor protein. J Biol Chem 273:33556–33560
10. Gotthardt M, Trommsdorff M, Nevitt MF, Shelton J, Richardson JA, Stockinger W, Nimpf J, Herz J (2000) Interactions of the low density lipoprotein receptor gene family with cytosolic adaptor and scaffold proteins suggest diverse biological functions in cellular communication and signal transduction. J Biol Chem 275:25616–25624
11. Barnes H, Larsen B, Tyers M, van der Geer P (2001) Tyrosine-phosphorylated low density lipoprotein receptor-related protein 1 (LRP1) associates with the adaptor protein SHC in SRC-transformed cells. J Biol Chem 276:19119–19125
12. Loukinova E, Ranganathan S, Kuznetsov S, Gorlatova N, Migliorini MM, Loukinov D, Ulery PG, Mikhailenko I, Lawrence DA, Strickland DK (2002) Platelet-derived growth factor (PDGF)-induced tyrosine phosphorylation of the low density lipoprotein receptor-related protein (LRP). Evidence for integrated co-receptor function between LRP and the PDGF. J Biol Chem 277:15499–15506
13. Su HP, Nakada-Tsukui K, Tosello-Trampont AC, Li Y, Bu G, Henson PM, Ravichandran KS (2002) Interaction of CED-6/GULP, an adapter protein involved in engulfment of apoptotic cells with CED-1 and CD91/low density lipoprotein receptor-related protein (LRP). J Biol Chem 277:11772–11779
14. Pietrzik CU, Yoon IS, Jaeger S, Busse T, Weggen S, Koo EH (2004) FE65 constitutes the functional link between the low-density lipoprotein receptor-related protein and the amyloid precursor protein. J Neurosci 24:4259–4265
15. van Kerkhof P, Lee J, McCormick L, Tetrault E, Lu W, Schoenfish M, Oorschot V, Strous GJ, Klumperman J, Bu G (2005) Sorting nexin 17 facilitates LRP recycling in the early endosome. EMBO J 24:2851–2861
16. Martin AM, Kuhlmann C, Trossbach S, Jaeger S, Waldron E, Roebroek A, Luhmann HJ, Laatsch A, Weggen S, Lessmann V, Pietrzik CU (2008) The functional role of the second NPXY motif of the LRP1 beta-chain in tissue-type plasminogen activator-mediated activation of *N*-methyl-D-aspartate receptors. J Biol Chem 283:12004–12013
17. Li Y, van Kerkhof P, Marzolo MP, Strous GJ, Bu G (2001) Identification of a major cyclic AMP-dependent protein kinase A phosphorylation site within the cytoplasmic tail of the low-density lipoprotein receptor-related protein: implication for receptor-mediated endocytosis. Mol Cell Biol 21:1185–1195
18. Barnes H, Ackermann EJ, van der Geer P (2003) v-Src induces Shc binding to tyrosine 63 in the cytoplasmic domain of the LDL receptor-related protein 1. Oncogene 22:3589–3597
19. Ranganathan S, Liu CX, Migliorini MM, Von Arnim CA, Peltan ID, Mikhailenko I, Hyman BT, Strickland DK (2004) Serine and threonine phosphorylation of the low density lipoprotein receptor-related protein by protein kinase Calpha regulates endocytosis and association with adaptor molecules. J Biol Chem 279:40536–40544
20. Betts GN, van der Geer P, Komives EA (2008) Structural and functional consequences of tyrosine phosphorylation in the LRP1 cytoplasmic domain. J Biol Chem 283:15656–15664
21. Jaeger S, Pietrzik CU (2008) Functional role of lipoprotein receptors in Alzheimer's disease. Curr Alzheimer Res 5:15–25
22. Herz J, Clouthier DE, Hammer RE (1992) LDL receptor-related protein internalizes and degrades uPA-PAI-1 complexes and is essential for embryo implantation. Cell 71:411–421
23. Herz J, Clouthier DE, Hammer RE (1993) Correction: LDL receptor-related protein internalizes and degrades uPA-PAI-1 complexes and is essential for embryo implantation. Cell 73:428
24. Rohlmann A, Gotthardt M, Hammer RE, Herz J (1998) Inducible inactivation of hepatic LRP gene by cre-mediated recombination confirms role of LRP in clearance of chylomicron remnants. J Clin Invest 101:689–695

25. Boucher P, Gotthardt M, Li WP, Anderson RG, Herz J (2003) LRP: role in vascular wall integrity and protection from atherosclerosis. Science 300:329–332
26. May P, Rohlmann A, Bock HH, Zurhove K, Marth JD, Schomburg ED, Noebels JL, Beffert U, Sweatt JD, Weeber EJ, Herz J (2004) Neuronal LRP1 functionally associates with postsynaptic proteins and is required for normal motor function in mice. Mol Cell Biol 24:8872–8883
27. Hu L, Boesten LS, May P, Herz J, Bovenschen N, Huisman MV, Berbee JF, Havekes LM, van Vlijmen BJ, Tamsma JT (2006) Macrophage low-density lipoprotein receptor-related protein deficiency enhances atherosclerosis in ApoE/LDLR double knockout mice. Arterioscler Thromb Vasc Biol 26:2710–2715
28. Roebroek AJ, Reekmans S, Lauwers A, Feyaerts N, Smeijers L, Hartmann D (2006) Mutant Lrp1 knock-in mice generated by recombinase-mediated cassette exchange reveal differential importance of the NPXY motifs in the intracellular domain of LRP1 for normal fetal development. Mol Cell Biol 26:605–616
29. Pietrzik CU, Busse T, Merriam DE, Weggen S, Koo EH (2002) The cytoplasmic domain of the LDL receptor-related protein regulates multiple steps in APP processing. Embo J 21:5691–5700
30. Willnow TE, Herz J (1994) Genetic deficiency in low density lipoprotein receptor-related protein confers cellular resistance to *Pseudomonas* exotoxin A. Evidence that this protein is required for uptake and degradation of multiple ligands. J Cell Sci 107:719–726
31. Hammond C, Helenius A (1994) Quality control in the secretory pathway: retention of a misfolded viral membrane glycoprotein involves cycling between the ER, intermediate compartment, and Golgi apparatus. J Cell Biol 126:41–52
32. Dedieu S, Langlois B, Devy J, Sid B, Henriet P, Sartelet H, Bellon G, Emonard H, Martiny L (2008) LRP-1 silencing prevents malignant cell invasion despite increased pericellular proteolytic activities. Mol Cell Biol 28:2980–2995
33. Herz J, Goldstein JL, Strickland DK, Ho YK, Brown MS (1991) 39-kDa protein modulates binding of ligands to low density lipoprotein receptor-related protein/alpha 2-macroglobulin receptor. J Biol Chem 266:21232–21238
34. Gordts PL, Reekmans S, Lauwers A, Van Dongen A, Verbeek L, Roebroek AJ (2009) Inactivation of the LRP1 intracellular NPxYxxL motif in LDLR-deficient mice enhances postprandial dyslipidemia and atherosclerosis. Arterioscler Thromb Vasc Biol 29:1258–1264
35. Nahari T, Barzilay E, Hirschberg K, Neumann D (2008) A transplanted NPVY sequence in the cytosolic domain of the erythropoietin receptor enhances maturation. Biochem J 410:409–416